Speciation of Nitrogen Containing Aromatics by Atmospheric Pressure Photoionization or Electrospray Ionization Fourier Transform Ion Cyclotron Resonance Mass Spectrometry

Jeremiah M. Purcell,* Ryan P. Rodgers,* Christopher L. Hendrickson,* and Alan G. Marshall*

National High Magnetic Field Laboratory, Florida State University, Tallahassee, Florida, USA

We determine the elemental compositions of aromatic nitrogen model compounds as well as a petroleum sample by atmospheric pressure photoionization (APPI) and electrospray Ionization (ESI) with a 9.4 Tesla Fourier transform ion cyclotron resonance (FT-ICR) mass spectrometer. From the double-bond equivalents calculated for the nitrogen-containing ions from a petroleum sample, we can infer the aromatic core structure (pyridinic versus pyrrolic nitrogen heterocycle) based on the presence of $M^{+\cdot}$ (odd-electron) versus $[M+H]^+$ (even-electron) ions. Specifically, nitrogen speciation can be determined from either a single positive-ion APPI spectrum or two ESI (positive- and negative-ion) spectra. APPI operates at comparatively higher temperature than ESI and also produces radical cations that may fragment before detection. However, APPI fragmentation of aromatics can be eliminated by judicious choice of instrumental parameters.   (J Am Soc Mass Spectrom 2007, 18, 1265–1273) © 2007 American Society for Mass Spectrometry

Complex organic mixture characterization by mass analysis requires the ultrahigh mass resolving power of Fourier transform ion cyclotron resonance mass spectrometry (FT-ICR MS) [1] to distinguish thousands of ionic species simultaneously [2, 3]. Electrospray ionization (ESI) of polar analytes typically involves proton transfer reactions that selectively ionize acids (to produce negative $[M-H]^-$ ions) or bases (to produce positive $[M+H]^+$ ions) [3–6]. The ionization efficiency correlates with acidity or basicity. For example, carboxylic acids are efficiently ionized by negative-ion ESI, whereas basic species (e.g., pyridinic N_1 species) are efficiently ionized by positive-ion ESI.

For non-polar aromatics, atmospheric pressure photoionization [7, 8] (APPI) can produce ions from species that are not efficiently ionized by ESI. The youngest of the soft ionization methods, dopant-assisted APPI, was initially developed to interface liquid chromatography to mass spectrometry to analyze simple mixtures. The ionization technique is ideal for non-polar aromatic compounds because the photon energy (typically 10 eV) is great enough to ionize aromatics but not non-

aromatic solvents. However, direct photoionization is usually not efficient [9] and the addition of a dopant enhances ionization efficiency through proton-transfer reactions and charge-exchange reactions.

Although APPI is considered to be a soft ionization technique (i.e., produces minimal fragmentation of most analytes), it has been considered less soft than ESI because the APPI heated nebulizer and the source region can reach >300 °C, whereas ESI is conducted at room temperature. Furthermore, toluene dopant-assisted APPI produces radical cations [10] that can participate in further gas-phase reactions.

Here, we compare ESI and APPI for analysis of petroleum crude oil (chosen because it represents the most complex organic mixture within a dynamic range of 1000–10,000). The nitrogen atom in aromatic N_1 class species in petroleum can reside in a five-membered ring (pyrrolic) or six-membered ring (pyridinic) and be readily protonated (pyridinic) or deprotonated (pyrrolic) by positive-ion or negative-ion ESI, respectively [11]. However, positive-ion APPI efficiently generates both pyrrolic and pyridinic nitrogen signals in a single mass spectrum [12].

APPI can extend the characterization of the petroleome [2, 3] to include non-polar aromatic species and enhance the extent of molecular speciation for better understanding of petroleum processing and refining. The nitrogen class species are efficiently ionized by both

ESI and APPI, and therefore offer a good basis for comparison. In this work, we couple APPI and ESI to a 9.4 Tesla FT-ICR mass spectrometer [13] for detailed compositional comparison of the ions produced from the same South American crude oil.

Experimental

South American Crude Oil

South American crude oil was supplied by ExxonMobil Research and Engineering Company (Annandale, NJ, USA) and a sample (2.8 g) was fractionated according to the saturates–aromatics–resins–asphaltenes (SARA) method [14]. The SARA method produced an aromatic fraction solution of 100 mg/mL in toluene. Two serial dilutions yielded a 2 mg/mL solution that was further diluted in toluene to 1 mg/mL for APPI analysis and 1 mg/mL in toluene:methanol (1:1 vol/vol) for ESI analysis.

Nitrogen Class Compounds

Five aromatic nitrogen compounds (acridine, carbazole, 7,9-dimethylbenz[c]acridine, 7H-dibenzo[c,g]carbazole and ellipticine) were purchased from Sigma–Aldrich (St. Louis, MO, USA). Equimolar solutions (2 mM) of the five nitrogen compounds were prepared in toluene. For ESI, the 2 mM solutions were diluted by a factor of 5 in toluene to 400 μM and, subsequently, equal aliquots (100 μL) of the five compound solutions were combined and diluted with methanol (1:1 vol/vol) to produce a final concentration of 40 μM for each compound. For APPI, equal aliquots (2 mL) of 2 mM solutions were combined to yield 400 μM (10 mL) for each compound, followed by a 1:10 dilution to 40 μM for each analyte.

FT-ICR Mass Spectrometry

With our previously described 9.4 T FT-ICR mass spectrometer [13, 15] and experimental conditions [12], multiple (100–200) time-domain acquisitions were averaged for each sample, Hanning-apodized, and zero-filled once before fast Fourier transform and magnitude calculation [16]. Negative-ion data were collected with similar parameters and appropriate polarity changes. All observed ions were singly charged, based on the unit m/z separation between $^{12}C_n$ and $^{13}C_1{}^{12}C_{n-1}$ isotopic variants of the same elemental composition [17]. Therefore, all mass spectral peaks are reported in Daltons rather than m/z.

APPI Conditions

The APPI source was supplied by ThermoFisher Scientific (San Jose, CA, USA). The vaporized analyte gas stream flows orthogonal to the mass spectrometer inlet (heated metal capillary) and the krypton vacuum UV lamp. The source was mounted to a custom-built interface to the first differentially pumped stage of the 9.4 Tesla FT-ICR mass spectrometer through a heated metal capillary [stainless steel, 750-μm inner diameter (i.d.)]. A Harvard stainless steel syringe (8 mL) and syringe pump delivered solution to the heated nebulizer of the APPI source. In the APPI source, solvent flow rate was 50–100 μL/min; the nebulizer heater was operated at 250–350 °C with carbon dioxide as the sheath gas at 550 kPa and the auxiliary gas port was plugged [12].

ESI Conditions

One end of a 50-μm i.d. fused silica tube was ground to a point and used as the microelectrospray source [18] to produce electrosprayed positive and negative ions. General conditions were: needle voltage, 2 kV (−2 kV negative-ion electrospray); tube lens, 350 V (−350 V negative-ion electrospray); and heated metal capillary current, 4.0 amperes. ESI negative-ion conditions were comparable to ESI positive-ion conditions.

Table 1. Homologous series of ions from a crude oil. Members of the series have the same N_1S_1 heteroatoms and the same calculated DBE value of 17.5, but differ in the number of CH_2 groups. Each molecular formula (from which the DBE value is calculated from Eq. 1) is for an $(M+H)^+$ ion, not its neutral precursor.

Carbon Number	Experimental Mass (Da)	DBE	Molecular Formula	Class	Calculated Mass (Da)	Error ppm
28	406.16243	17.5	$C_{28}H_{24}N_1S_1$	N_1S_1	406.16240	0.08
29	420.17804	17.5	$C_{29}H_{26}N_1S_1$	N_1S_1	420.17805	-0.02
30	434.19366	17.5	$C_{30}H_{28}N_1S_1$	N_1S_1	434.19370	-0.09
31	448.20934	17.5	$C_{31}H_{30}N_1S_1$	N_1S_1	448.20935	-0.02
32	462.22501	17.5	$C_{32}H_{32}N_1S_1$	N_1S_1	462.22500	0.03
33	476.24063	17.5	$C_{33}H_{34}N_1S_1$	N_1S_1	476.24065	-0.04
34	490.25633	17.5	$C_{34}H_{36}N_1S_1$	N_1S_1	490.25630	0.07
35	504.27200	17.5	$C_{35}H_{38}N_1S_1$	N_1S_1	504.27195	0.10
36	518.28764	17.5	$C_{36}H_{40}N_1S_1$	N_1S_1	518.28760	0.08
37	532.30328	17.5	$C_{37}H_{42}N_1S_1$	N_1S_1	532.30325	0.06
38	546.31905	17.5	$C_{38}H_{44}N_1S_1$	N_1S_1	546.31890	0.28
39	560.33465	17.5	$C_{39}H_{46}N_1S_1$	N_1S_1	560.33455	0.18

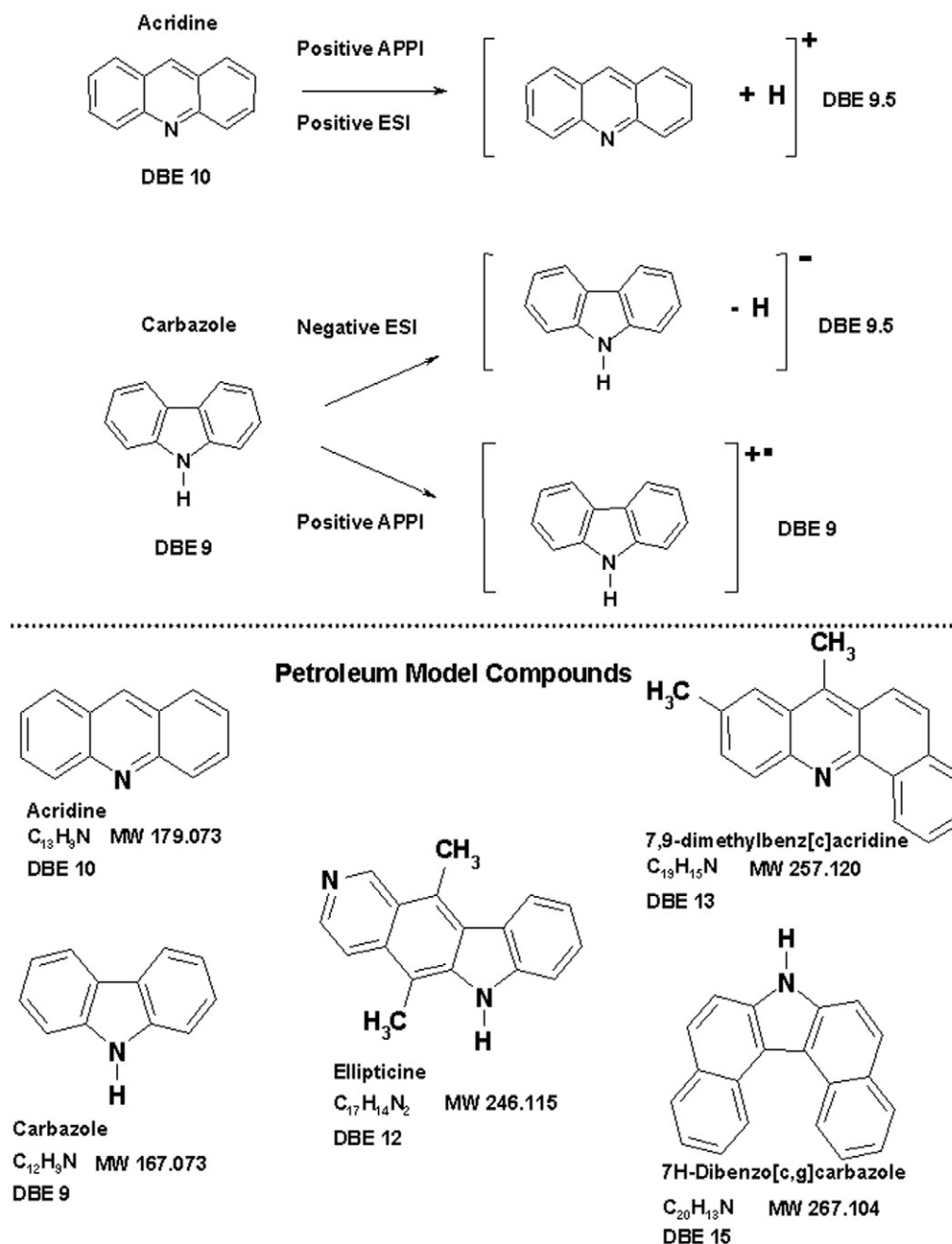**Figure 1.** ESI and APPI ionization pathways for acridine and carbazole (top) and nitrogen class compounds (bottom). For ESI, negative-ion and positive-ion spectra would be necessary to detect both species. However, both compounds yield APPI positive ions. Double-bond equivalents (DBE) are calculated from eq 1 for each ion. For the nitrogen class compounds, carbazole and 7H-dibenzo-[c,g]carbazole are pyrrolic (acidic), whereas acridine and 7,9-dimethylbenz[c]acridine are pyridinic (basic) species. Ellipticine, with two nitrogen heteroatoms, has both pyrrolic and pyridinic moieties.
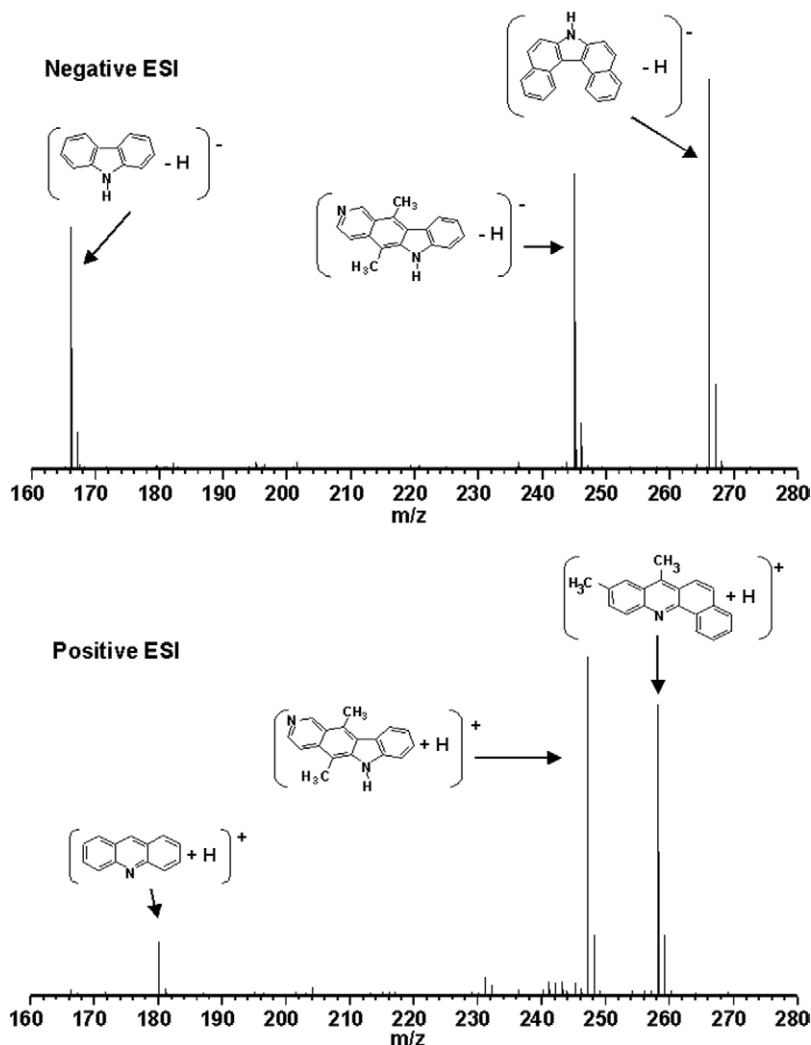
Figure 2. Negative-ion and positive-ion ESI FT-ICR mass spectra of representative nitrogen-class compounds. For both spectra, an equimolar solution was electrosprayed. The pyrrolic species were ionized by negative-ion ESI and the pyridinic species by positive-ion ESI. Ellipticine was detected in both negative-ion and positive-ion spectra.

Double-Bond Equivalents Calculation

Crude oil consists primarily of homologous series. Each homologous series is categorized by heteroatom class ($N_nO_oS_s$), double-bond equivalents (DBE; see eq 1), and carbon number. The DBE is equal to the number of rings plus double bonds and is calculated from [19]

$$DBE(C_cH_hN_nO_oS_s) = c - (h/2) + (n/2) + 1 \qquad (1)$$

Within each heteroatom class, there are many DBE values. For example, $C_{42}H_{59}N_1$ belongs to the N_1 class with DBE = 14, whereas $C_{42}H_{53}N_1$ belongs to the same heteroatom class, N_1, but its DBE is 17. Table 1 shows the carbon number distribution (28–39) for the homologous members of the N_1S_1 class with DBE 17.5 (pyridinic). All DBE values in this work are calculated from the molecular formula of the ion, so that odd-electron radical cations have integer DBE values, whereas pro-tonated or deprotonated (even-electron) ions have half-integer DBE values.

Results and Discussion

Nitrogen Compounds

Figure 1 (top) shows the possible ionization pathways for aromatic N_1 class compounds (acridine and carbazole) by APPI (positive-ion) and ESI (negative-ion and positive-ion). The two pathways involving proton transfer yield even-electron $[M+H]^+$ or $[M-H]^-$ ions with half-integer DBE values. Positive-ion APPI can also form odd-electron radical cations with integer DBE values.

Five nitrogen-containing aromatics (Figure 1, bottom) were selected as petroleum model compounds: two pyrrolic (five-membered ring), two pyridinic (six-membered ring), and one with one of each ring
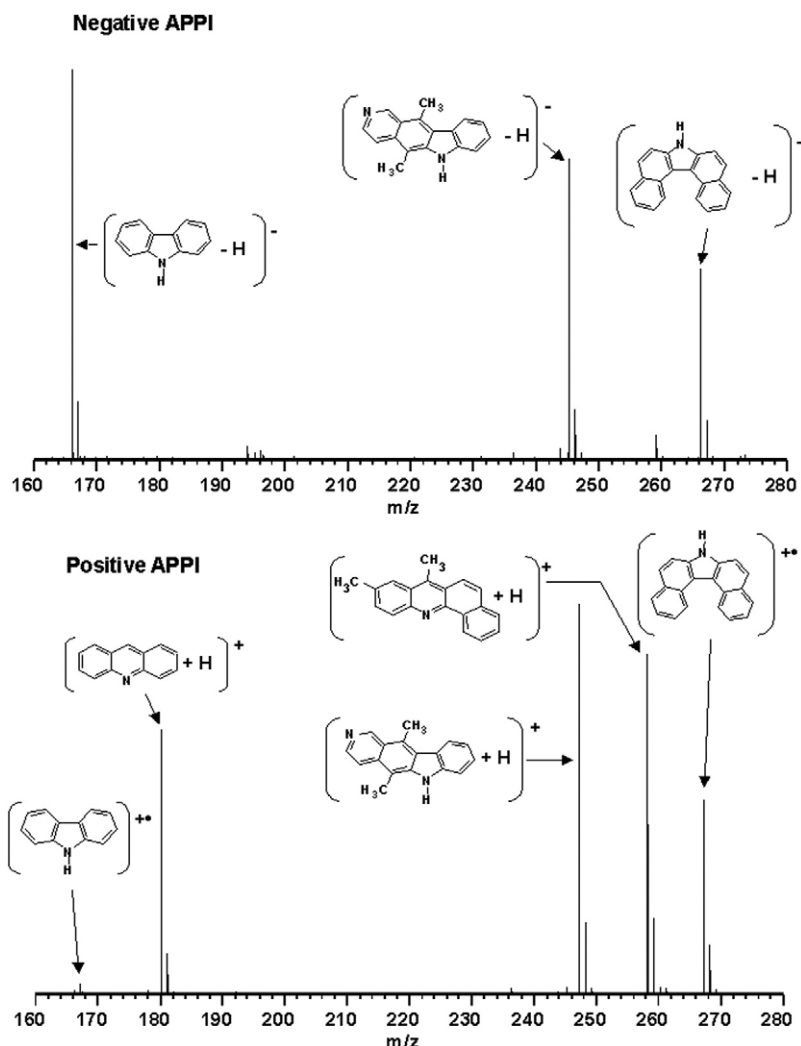
Figure 3. Negative-ion and positive-ion APPI spectra of representative nitrogen-class compounds. For both spectra, an equimolar solution was infused into the APPI source. The pyrrolic species were detected in the negative-ion APPI spectrum, and all five compounds were detected in the positive-ion APPI spectrum.

type° (ellipticine).° Figure° 2° shows° the° positive-ion (bottom) and negative-ion (top) ESI spectra of an equimolar solution of the nitrogen compounds. The pyrrolic nitrogen species deprotonate to form $[M-H]^-$ ions, whereas the pyridinic species protonate to form $[M+H]^+$ ions.

Figure°3°shows°positive-ion°(bottom)°and°negative-ion (top) APPI spectra of an equimolar solution of the nitrogen compounds. Both positive and negative ions are formed simultaneously in the source, enabling detection of either positive or negative ions by appropriate instrument polarity changes and no source interruption. The APPI negative-ion spectrum shows the deprotonated pyrrolic species. However, in the APPI positive-ion spectrum, all five nitrogen compounds are detected simultaneously. The pyrrolic species form radical molecular ions and the pyridinic species form protonated compounds.

The pyrrolic compounds (carbazole and 7H-dibenzo-[c,g]carbazole) exhibit different ionization efficiency (and ion type) in negative-ion and positive-ion APPI mass°spectra.°Carbazole°(7.6°eV°ionization°energy)°[20] forms radical molecular cations less efficiently than the more extensively conjugated 7H-dibenzo[c,g]carbazole (7.1°eV°ionization°energy)°[20].°In°contrast,°APPI°generates much more similar $[M-H]^-$ ion abundances for both°carbazoles°(Figure°3,°top).

Nitrogen Class Speciation

Figure°4°is°the°positive-ion°APPI°broadband°mass spectrum of a South American crude oil, including various closely spaced mass doublets. First, a 3.4 mDa°separation°(zoom°inset°in°Figure°4)°results°from two compounds that differ in elemental composition by C_3 versus SH_4, a common mass doublet for crude oil. That mass difference is also seen by electrospray
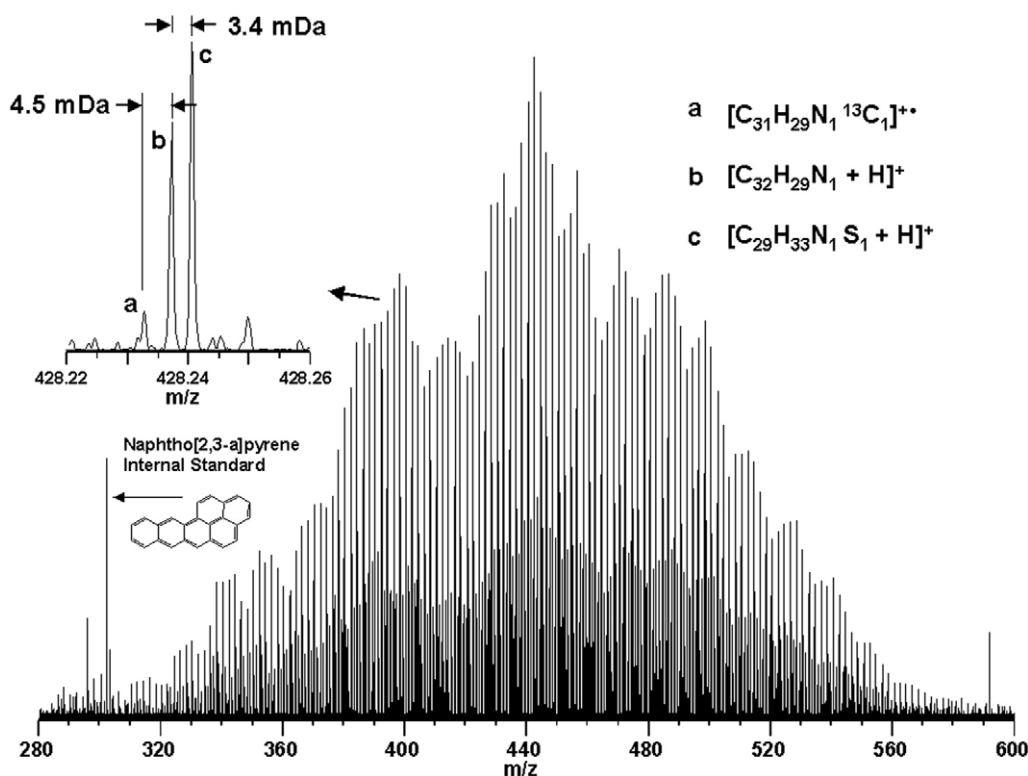
Figure 4. Positive-ion APPI FT-ICR broadband mass spectrum of a South American crude oil. Both radical molecular ions and protonated compounds are formed in the APPI source. The mass scale-expanded inset shows two common spectral peak doublets for APPI. Naphtho[2,3-a]pyrene was added to the petroleum sample to test for possible fragmentation. No fragment ions were observed.

ionization because both species can produce protonated compounds.

Second, APPI can produce an additional 4.5 mDa (^{13}C versus ^{12}CH) doublet not seen by ESI, as a result of formation of both a radical molecular ion ($M^{+\bullet}$) and protonated molecule ($[M+H]^+$) from the same neutral precursor. Naphtho[2,3-a]pyrene was added as a standard to test for fragmentation (see below); i.e., no spectral peaks corresponding to loss of one or two hydrogen atoms from naphtho[2,3-a]pyrene were observed.

The spectral peaks from the broadband spectrum were assigned unique molecular formulas based on accurate mass measurement for homologous series [21]. Similar broadband spectra were acquired (data not shown) for both positive-ion and negative-ion ESI. The N_1 class ions were sorted by DBE and carbon number. Figure 5 shows DBE distributions for APPI positive-ion nitrogen class species and ESI negative- and positive-ion nitrogen classes.

The DBE values in Figure 5 were calculated from eq 1 for the ion molecular formulas. Accordingly, half-integer DBE values result for even-electron (protonated or deprotonated compound) ions, $[M+H]^+$ or $[M-H]^-$, whereas integer DBE values result for odd-electron ions (e.g., radical cations, $M^{+\cdot}$). Thus, the DBE value calculated from eq 1 for any N_1-class aromatic compound readily distinguishes even-electron (pyridinic, half-

integer DBE) from odd-electron (pyrrolic, integer DBE) ions produced by APPI.

From the DBE distribution (Figure 5, top), clearly APPI produces both protonated compounds (half-integer DBE) and radical molecular ions (integer DBE). Interestingly, the radical molecular ions begin at DBE 9, the same DBE threshold observed for negative even-electron $[M-H]^-$ ions. In fact, if the negative-ion ESI DBE distributions are shifted one-half DBE lower (to compensate for the one-proton difference in mass between $[M-H]^-$ and $M^{+\cdot}$), then the negative- and positive-ion ESI DBE distributions are essentially the same as the combined $[M+H]^+$ and $M^{+\cdot}$ distribution from APPI.

Table 2 lists the elemental compositions assigned to the APPI positive N_1-class ions (DBE 9, pyrrolic) and ESI negative N_1-class ions (DBE 9.5, pyrrolic). Note that the neutral molecular formulas are the same for both kinds of ions. The same behavior is seen throughout the nitrogen class DBE distributions—that is, the neutral elemental compositions inferred from the deprotonated (negative-ion) ESI ions are also seen for the positive-ion APPI ions at one-half integer lower DBE. Furthermore, the relative DBE abundances (APPI DBE 9 versus ESI DBE 9.5; Figure 5) agree with the nitrogen class compound spectra (Figures 2 and 3)—that is, a carbazole type
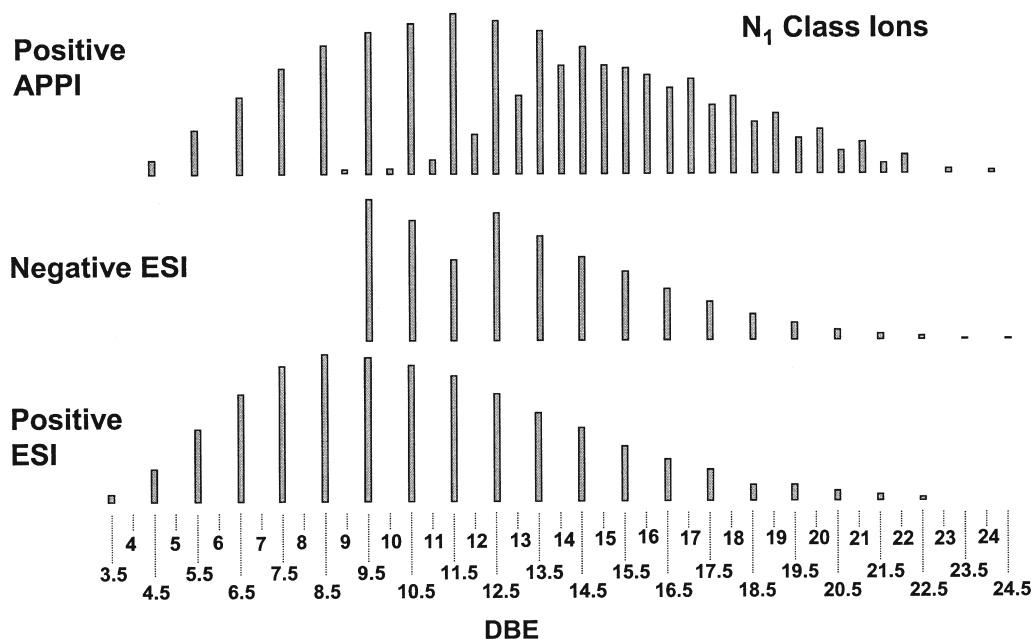
Figure 5. ESI (positive-ion and negative-ion) and APPI (positive-ion) DBE distributions for the N_1 class from the petroleum sample. The ion DBE is calculated from eq 1. The total relative ion abundance for each DBE is plotted on the y-axis. For ESI, protonation or deprotonation yields ions of half-integer DBE values. For APPI, radical molecular ions yield integer DBE values. Note that positive-ion APPI can distinguish pyridinic $(M+H)^+$ from pyrrolic $(M^{+\cdot})$ nitrogen ions based on their respective half-integer and integer DBE values.

core structure compound will form a radical molecular ion (APPI positive-ion, 9 DBE) less efficiently (Figure 3, bottom) than in negative-ion ESI (9.5 DBE) (Figure 2, top). Moreover, as the DBE increases for the pyrrolic species (which form radical molecular ions, integer DBE) in the positive-ion APPI DBE distribution, the relative DBE abundance also increases in agreement with the nitrogen compound spectra.

Ion Fragmentation

Ion dissociation is more prevalent in APPI than ESI because of hot gases and radical ion formation. Fragmentation can be minimized (or eliminated) by proper

choice of source pressure and tube lens voltage. The APPI source interfaces with the first stage of the mass spectrometer through a heated metal capillary (HMC) mounted to a custom-built adapter. At the exit of the HMC, an open-ended cylindrical tube (tube lens) focuses the ion flux in front of a conical skimmer. The skimmer is a pressure conductance limit (1-mm orifice) between the first stage of the mass spectrometer and the second stage that houses the first octopole ion guide/trap. A convectron gauge senses the pressure in the first stage (~2.1 Torr for ESI conditions) and a direct current potential (350 V for ESI) is applied to the tube lens. Depending on the pressure and applied voltages in this region, ion fragmentation can ensue [22, 23].

Table 2. List of DBE 9 positive-ion N_1-class APPI species $(M^{+\cdot})$ and the DBE 9.5 negative-ion N_1-class ESI species $(M–H)^{-a}$

Experimental mass (Da)	Calculated error (ppm)	Ion molecular formula	DBE	Mass (Da)
APPI [M]^{+•}				
461.40162	0.04	$C_{33}H_{51}N_1$	9	461.4016
475.41720	−0.11	$C_{34}H_{53}N_1$	9	475.4173
489.43289	0.02	$C_{35}H_{55}N_1$	9	489.4329
503.44869	−0.27	$C_{36}H_{57}N_1$	9	503.4486
517.46428	0.15	$C_{37}H_{59}N_1$	9	517.4642
ESI [M–H]^−				
460.39483	−0.10	$C_{33}H_{50}N_1$	9.5	460.3949
474.41052	−0.01	$C_{34}H_{52}N_1$	9.5	474.4105
488.42610	−0.15	$C_{35}H_{54}N_1$	9.5	488.4262
502.44181	−0.03	$C_{36}H_{56}N_1$	9.5	502.4418
516.45748	0.01	$C_{37}H_{58}N_1$	9.5	516.4575

aEach molecular formula [and the DBE value computed from it (eq 1)] is for the stated ion, not its neutral precursor.
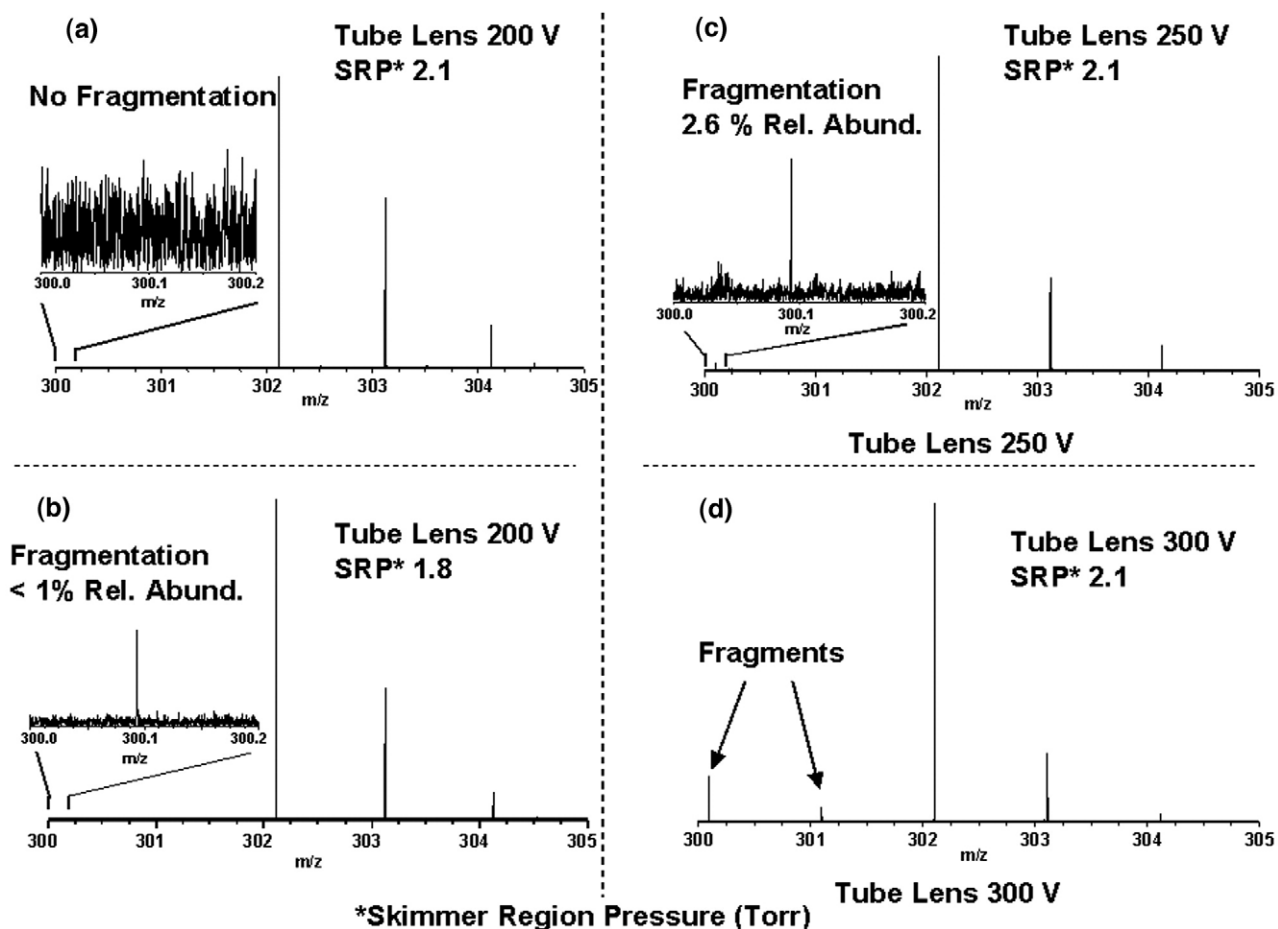
Figure 6. Positive-ion APPI FT-ICR mass spectra of naphtho[2,3-a]pyrene ($C_{24}H_{14}$, neutral monoisotopic mass, 302.110 Da) for various choices of tube lens voltage and skimmer region pressure. Fragmentation is evident at higher tube lens potential and/or lower pressure. At a tube lens potential of 200 V DC and a skimmer region pressure of 2.1 Torr, no fragmentation is observed.

The APPI source produces hot gas at the inlet of the HMC, resulting in elevated gas temperature in the first stage (skimmer region) of the mass spectrometer and reduced pressure. Furthermore, tube lens voltage >200 V in combination with increased temperature for APPI can cause significant fragmentation.

The mass spectra of naphtho[2,3,a]pyrene ($C_{24}H_{14}$) in Figure 6 at different skimmer region pressures and tube lens voltages illustrate fragmentation. In Figure 6a and b, the tube lens voltage is held constant and the skimmer region pressure is raised from 1.8 Torr (Figure 6b) to 2.1 Torr (Figure 6a) by partial valve closure at the vacuum pump. At 1.8 Torr, a fragmentation threshold is reached. The mass scale-expanded inset (Figure 6b) shows formation of $[C_{24}H_{12}]^{+\cdot}$, a fragment formed by the loss of two hydrogen atoms. In Figure 6c and d, the skimmer region pressure is maintained at 2.1 Torr and the tube lens voltage is varied. At increased tube lens voltage (Figure 6d), the loss of one hydrogen atom from the monoisotopic precursor, $[C_{24}H_{13}]^{+\cdot}$ at mass 301 Da is observed in addition to the loss of two hydrogen atoms (i.e., a 4.5 mDa doublet is seen at 301 Da).

Furthermore, under conditions at which fragmenta-

tion occurs (Figure 6b,c,d), the magnitude (zoom inset data not shown) of the $[C_{24}H_{14}+H]^{+}$ spectral peak relative to that of $[C_{24}H_{14}]^{+\cdot}$ decreases as fragmentation increases. All other spectra in this work were acquired under Figure 6A conditions.

Conclusions

Positive-ion APPI spectra yield the same information as combined positive- and negative-ion ESI spectra for N_1 class aromatics. Also, ESI and APPI mass analysis of a petroleum sample can yield aromatic core structural information. Although pyridinic and pyrrolic species ionization efficiency depends on the ionization method, APPI can generate positive ions for both pyridinic and pyrrolic compounds. The DBE values for the APPI positive-ion species differ by 0.5 for odd- and even-electron ions, and can distinguish pyrrolic from pyridinic nitrogen class species in a petroleum sample.

The APPI source uses a heated nebulizer (300 °C) to form gas-phase analytes and thus increases the thermal

energy of analyte and atmospheric gases in the source region. The increase in thermal energy changes the gas dynamics of the mass spectrometer and can induce fragmentation. Nevertheless, fragmentation of aromatics can be monitored and negated by proper choice of instrumental parameters. In this work, the good agreement in speciation of the aromatic nitrogen class species between a proven soft ionization technique (ESI) and APPI suggests that APPI can be conducted so as to virtually eliminate fragmentation.

Acknowledgments

References

1. Marshall, A. G.; Hendrickson, C. L.; Jackson, G. S. Fourier Transform Ion Cyclotron Resonance Mass Spectrometry: A Primer. *Mass Spectrom. Rev.* **1998,** *17,* 1–35.
2. Marshall, A. G.; Rodgers, R. P. Petroleomics: The Next Grand Challenge for Chemical Analysis. *Acc. Chem. Res.* **2004,** *37,* 53–59.
3. Rodgers, R.; Schaub, T.; Marshall, A. Petroleomics: MS Returns to Its Roots. *Anal. Chem.* **2005,** *77,* 20A–27A.
4. Zhan, D. L.; Fenn, J. B. Electrospray Mass Spectrometry of Fossil Fuels. *Int. J. Mass Spectrom.* **2000,** *194,* 197–208.
5. Rodgers, R. P.; Klein, G. C.; Stanford, L. A.; Kim, S.; Marshall, A. G. Characterization of Heavy, Biodegraded Crude Oils by High Resolution ESI FT-ICR Mass Spectrometry. *Am. Chem. Soc. Abstr.* **2004,** *228,* U654.
6. Rodgers, R. P.; Hendrickson, C. L.; Emmett, M. R.; Marshall, A. G. Reading Chemical Fine Print: Resolution and Identification of 3000 Nitrogen-containing Aromatic Compounds from a Single Electrospray Ionization Fourier Transform Ion Cyclotron Resonance Mass Spectrum of Heavy Petroleum Crude Oil. *Energy Fuels* **2001,** *15,* 492–498.
7. Robb, D. B.; Covey, T. R.; Bruins, A. P. Atmospheric Pressure Photoionization: An Ionization Method for Liquid Chromatography–Mass Spectrometry. *Anal. Chem.* **2000,** *72,* 3653–3659.
8. Syage, J. A.; Evans, M. D. Photoionization Mass Spectrometry. *Spectroscopy* **2001,** *16,* 14–21.
9. Tubaro, M.; Marotta, E.; Seraglia, R.; Traldi, P. Atmospheric Pressure Photoionization Mechanisms. 2. The Case of Benzene and Toluene. *Rapid Commun. Mass Spectrom.* **2003,** *17,* 2423–2429.
10. Raffaelli, A.; Saba, A. Atmospheric Pressure Photoionization Mass Spectrometry. *Mass Spectrom. Rev.* **2003,** *22,* 318–331.
11. Hughey, C. A.; Rodgers, R. P.; Marshall, A. G. Resolution of 11,000 Compositionally Distinct Components in a Single Electrospray Ionization Fourier Transform Ion Cyclotron Resonance Mass Spectrum of Crude Oil. *Anal. Chem.* **2002,** *74,* 4145–4149.
12. Purcell, J. M.; Hendrickson, C. L.; Rodgers, R. P.; Marshall, A. G. Atmospheric Pressure Photoionization Fourier Transform Ion Cyclotron Resonance Mass Spectrometry for Complex Mixture Analysis. *Anal. Chem.* **2006,** *78,* 5906–5912.
13. Senko, M. W.; Hendrickson, C. L.; Pasa-Tolic, L.; Marto, J. A.; White, F. M.; Guan, S.; Marshall, A. G. Electrospray Ionization Fourier Transform Ion Cyclotron Resonance at 9.4 T. *Rapid Commun. Mass Spectrom.* **1996,** *10,* 1824–1828.
14. Rudzinski, W. E.; Aminabhavi, T. M.; Sassman, S.; Watkins, L. M. Isolation and Characterization of the Saturate and Aromatic Fractions of a Maya Crude Oil. *Energy Fuels* **2000,** *14,* 839–844.
15. Håkansson, K.; Chalmers, M. J.; Quinn, J. P.; McFarland, M. A.; Hendrickson, C. L.; Marshall, A. G. Combined Electron Capture and Infrared Multiphoton Dissociation for Multistage MS/MS in a Fourier Transform Ion Cyclotron Resonance Mass Spectrometer. *Anal. Chem.* **2003,** *75,* 3256–3262.
16. Marshall, A. G.; Verdun, F. R. Fourier Transforms in NMR, Optical, and Mass Spectrometry: A User's Handbook; Elsevier: Amsterdam, 1990.
17. Senko, M. W.; Beu, S. C.; McLafferty, F. W. Automated Assignment of Charge States from Resolved Isotopic Peaks for Multiply Charged Ions. *J. Am. Soc. Mass Spectrom.* **1995,** *6,* 52–56.
18. Emmett, M. R.; Caprioli, R. M. Micro-Electrospray Mass Spectrometry: Ultra-high-sensitivity Analysis of Peptides and Proteins. *J. Am. Soc. Mass Spectrom.* **1994,** *5,* 605–613.
19. McLafferty, F. W.; Turecek, F. Interpretation of Mass Spectra; 4th ed.; University Science Books: Mill Valley, CA, 1993.
20. Rapp, U.; Staab, H. A.; Wunsche, C. NIST 2005 [*NIST/EPA/NIH Mass Spectral Library 2005* (Upgrade)]; Wiley: Hoboken, NJ, 2005.
21. Hughey, C. A.; Hendrickson, C. L.; Rodgers, R. P.; Marshall, A. G.; Qian, K. Kendrick Mass Defect Spectrum: A Compact Visual Analysis for Ultrahigh-Resolution Broadband Mass Spectra. *Anal. Chem.* **2001,** *73,* 4676–4681.
22. Hagman, C.; Tsybin, Y. O.; Håkansson, P. Solution-phase Deuterium/ Hydrogen Exchange at a Specific Residue Using Nozzle-Skimmer and Electron Capture Dissociation Mass Spectrometry. *Rapid Commun. Mass Spectrom.* **2006,** *20,* 661–665.
23. Loo, J. A.; Edmonds, C. G.; Smith, R. D. Tandem Mass-Spectrometry of Very Large Molecules—Serum-Albumin Sequence Information from Multiply Charged Ions Formed by Electrospray Ionization. *Anal. Chem.* **1991,** *63,* 2488–2499.